JOURNAL OF CATALYSIS **131**, 582–589 (1991)

Catalytic Oxidation of Carbon Monoxide over Superconducting $La_{2-x}Sr_xCuO_{4-\delta}$ Systems between 373–523 K

S. RAJADURAI,* J. J. CARBERRY,* B. LI,† AND C. B. ALCOCK†

**Laboratory of Catalysis, Department of Chemical Engineering, and †Center for Sensor Materials, Department of Materials Science and Engineering, University of Notre Dame, Notre Dame, Indiana 46556*

Received March 1, 1990; revised November 6, 1990

The catalytic oxidation of carbon monoxide on superconducting $La_{2-x}Sr_xCuO_{4-\delta}$ systems has been studied in the temperature range 373 to 573 K. These solid oxide solutions are found to show high catalytic activity for oxidation (carbon monoxide oxidation) which is comparable to that of a highly dispersed 0.5% Pt/alumina fume abatement catalyst. The kinetics of CO oxidation on these solid oxide solutions conforms to the same Langmuir–Hinshelwood model as that of the Pt/alumina catalyst. The catalytic activity which was studied as a function of Sr concentration (x) in these solid oxide solutions shows a "volcano" behavior with a maximum activity at $x = 0.4$. The variation of catalytic activity is compared and found to be concomitant with that of the variation of the electrical conductivity, lattice parameter, and oxygen vacancy concentration on the K_2NiF_4-type $La_{2-x}Sr_xCuO_{4-\delta}$ lattice and the thermodynamic activity of SrO.

INTRODUCTION

Among technological problems that require attention today are the chemical conversion of pollutants into innocuous gases, of coal into gas, of water into hydrogen and oxygen, and of air and water into fertilizers. As a consequence of the increased awareness of air pollution problems in developing countries, catalytic oxidation of CO has been intensely studied for the past few decades (*1–6*). Supported noble metal catalysts have been the standard and the most widely used catalysts for CO oxidation reaction (*7, 8*). Nevertheless, the high cost of the noble metals has encouraged the development of oxides, spinels, perovskites, and alloys of transition metals as potential catalysts for pollution abatement processes. Though several substitutes had been reported for Pt, the noble metal catalysts have not yet been replaced successfully (*9–11*), save for our recent report, which sets forth the discovery of La, Sr, and Cr solid oxide solutions which rival Pt in CO oxidation and reveal provocative activity in olefin hydrogenation (*1*).

Insofar as these formulations are of the superconducting class, it would follow that "normal" conductivity would be manifest at temperatures typical of catalytic activity. Inspired by the established teaching that catalysis, in the large, is often associated with electron exchange twixt the solid catalyst and reactant(s), we deemed it appropriate that solid oxide solutions of the superconducting category be further evaluated as catalyst candidates which might rival conventional (metal) conductors. In the present program the catalytic behavior of a series of solid oxide solutions of La, Sr, and Cu has been studied.

$La_{2-x}Sr_xCuO_{4-\delta}$ is a K_2NiF_4-type solid oxide solution characterized by the intergrowth of perovskite and sodium chloride type layers illustrated in Fig. 1. The high electronic conductivity of these compounds is due to the ability of copper to take different coordinations as well as the formation of mixed valence states. The formation of solid oxide solutions with alkaline earth metal oxides in a wide range ($0 < x < 1$ in the case of SrO) is a significant property of these compounds. In this article we discuss

0021-9517/91 $3.00

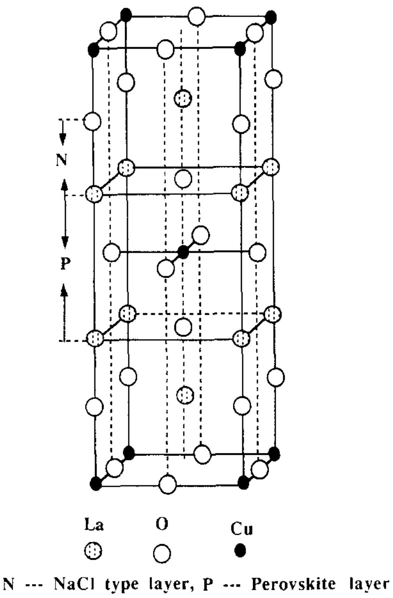

FIG. 1. K_2NiF_4-type structure for La_2CuO_4 solid oxide solution.

the role that these K_2NiF_4-type $La_{2-x}Sr_xCuO_{4-\delta}$ oxides (superconductors at low temperatures) might exhibit as catalysts. And, logically, said catalytic activity should be explored in terms of the conductivity of these formulations.

PREPARATION OF THE CATALYST

Solid oxide solutions of $La_{2-x}Sr_xCuO_{4-\delta}$ ($0 < x < 1$) were prepared by the conventional ceramic technique. The constituents were thoroughly mixed in the proper ratio and pellets were prepared by pressing these mixtures. Each pellet was sintered in an alumina crucible under air for 12 hr at 1323 K. Cycles of grinding, pelletizing, and heating were repeated three times on each sample to ensure complete reaction. The pellets were cooled to 873 K in air inside the furnace and then cooled to room temperature outside the furnace. X-ray diffraction, SEM, and EDX showed that each sample was a *homogeneous single phase*. All the component oxides used were 99.99% Puratronic specialty products from AESAR (Johnson Matthey). A uniform range of mesh sizes of powder (the sieve fraction between 10 and 35 μm) were used for the catalytic studies. The surface area of the solid solutions was measured by the BET N_2 physical adsorption technique and found to be typically ≤0.4 m^2/g.

EXPERIMENTAL

Temperature-programmed catalytic studies were carried out in the Notre Dame multifunctional *in situ* catalyst characterization unit (*12*). Tests were made with a fixed feed concentration of the gas mixture (1% CO in oxygen) through a fixed amount of powdered catalyst (0.25 g) to maintain constant contact time. The conversion of CO was determined as a function of temperature while the catalyst was programmably heated (2°C min). The effluent from the gradientless recycling reactor was sampled using a zero volume sampling valve at different time intervals and the sample was analyzed by means of a gas liquid chromatograph interphased with an automatic integrator.

Independent thermogravimetric analyses were conducted with a Cahn TGA 113 system under controlled atmosphere to establish the value of δ (deviation from stoichiometry) for each sample. The details of the measurements are available elsewhere (*13, 14*). A known amount of the sample pellet (<100 mg) was mounted on a platinum crucible so that it made contact only with the thin edge of the crucible. Each sample was reduced under a hydrogen and argon gas mixture after equilibration with a known oxygen partial pressure. No interaction between the sample and Pt was observed in our experimental conditions. The variation of the oxygen content in the solid oxide solutions was determined from 823 to 1323 K under an oxygen partial pressure from 10^5 (pure oxygen) to 6.6 Pa. Blank experiments were carried out with predried alumina powder in the same crucible before and after the investigation of the sample to check the effects of temperature and different gas mixtures on the buoyancy. MKS mass controllers were used to control the flowing gas mixtures. Oxygen partial pressures were monitored with a Y_2O_3-stabilized ZrO_2 cell placed in a furnace which was upstream from the microbalance.

The thermodynamic activity of SrO of these solid solutions was studied with a solid state electrochemical technique using calcium fluoride single crystal as the electrolyte. A typical SrO concentration cell was assembled as follows:

$$O_2, Pt|SrO + SrF_2|CaF_2|La_{2-x}Sr_xCuO_{4-\delta} + SrF_2|Pt,O_2.$$

Extra dry grade oxygen was passed through this electrochemical cell to establish the oxygen potential of the atmosphere. The overall composition of each electrode was made from equimolar amounts of the respective components. The electrodes were prepared by the conventional method, i.e., the solid solutions were synthesized first by sintering pellets of appropriate mixtures of the component oxides at 1323 K, then the electrode pellets were prepared from these compounds. The emf measurements were carried out in several cycles of increasing and decreasing temperatures from 900 to 1200 K. The thermodynamic activity of SrO was calculated using the Nernst equation (*13, 14*). The time to reach a steady emf was about 4–24 hr. The achievement of equilibrium emf values in each cell was assured by temporarily polarizing the cell with an external battery; the emf returned to the original values within ±1.5 mV in a period of time after the polarization ceased depending on the experimental condition. Both electrode and electrolyte were checked by x-ray diffraction before and after emf measurements and no significant reaction was found.

RESULTS AND DISCUSSION

Various combinations of the solid oxide solutions of La, Sr, and Cu of the formula $La_{2-x}Sr_xCuO_{4-\delta}$ $(0 < x < 1)$ were prepared and the kinetics of the catalytic oxidation of CO on these solid solutions were studied.

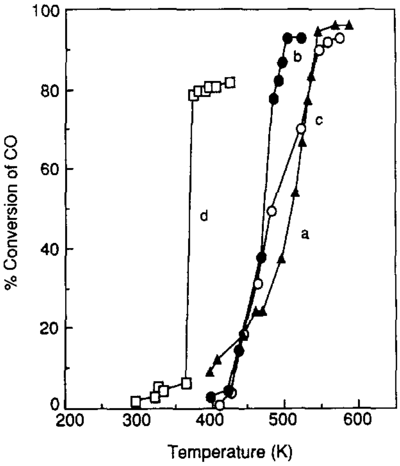

FIG. 2. Representative LOT curves for solid oxide solutions (a) Sr = 0, (b) Sr = 0.1, (c) Sr = 1.0, and (d) Pt/alumina catalyst.

(*Note: these samples were free of contact with Pt.*) The kinetics of CO oxidation on these solid solutions follow the Langmuir–Hinshelwood model as in the case of supported noble metal catalyst (Pt/alumina). The "light-off" temperature curve (% CO conversion versus temperature) for the solid oxide solutions is compared with that of the Pt/alumina catalyst to show the similarity in the CO oxidation behavior in Fig. 2. The LOT results provide support for the Pt-like oxidation behavior of the solid solutions. However, the LOT is higher for the solid oxide solutions than for the Pt catalyst, but the oxides do not sinter significantly. Sintering is known to decrease the activity of the Pt catalyst. The catalytic activity, as measured by the percentage conversion at a constant temperature (475 K) and at a fixed contact time for a constant amount of catalyst (0.25 g), of the solid oxide solutions of $La_{2-x}Sr_xCuO_{4-\delta}$ versus Sr concentration (x) is given in Fig. 3. The catalytic activities of these solid oxide solutions are compared with that of the component individual oxides CuO, SrO, and La_2O_3. The solid oxide solutions show significant differences in catalytic activity from that of the individual oxides. The

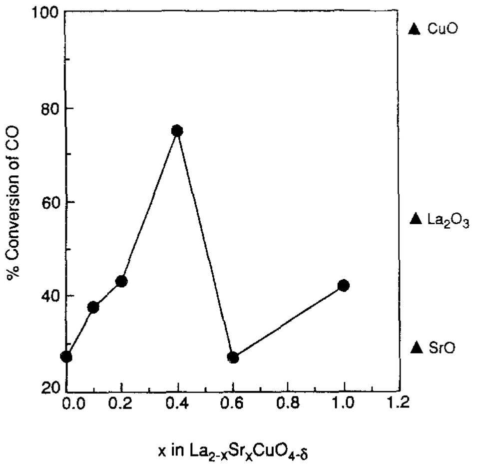

FIG. 3. Percentage conversion of CO as a function of Sr concentration in $La_{2-x}Sr_xCuO_{4-\delta}$ at 475 K.

"volcano" plot of Fig. 3 reveals three areas of catalytic activity as a result of increasing Sr^{2+} in the place of a La^{3+} in the La_2CuO_4 matrix:

(a) a sharp increase of activity caused by the replacement of La^{3+} by Sr^{2+} with ($0 < x < 0.4$),

(b) a sharp fall in activity with further increase in Sr^{2+} substitution ($0.4 < x < 0.6$),

(c) increasing or constant activity in the region $x > 0.6$.

The replacement of La^{3+} by Sr^{2+} in the sublattice of K_2NiF_4-type structure of La_2CuO_4 leads to several possibilities for the charge balance and defect formation in the copper cation sublattice and in the oxygen anion sublattice. Oxygen vacancy creation by Sr^{2+} substitution in the K_2NiF_4 lattice is represented by Kroger–Vink notation as follows:

$$SrO \rightarrow Sr'_{La} + O_o + 1/2\ V''_o. \qquad (1)$$

The oxygen defects formed in the K_2NiF_4-type oxide lattice lead to an increase in the lattice parameter due to the displacement of the oxygen atoms from their ideal position, which is sufficient to produce structural distortion in the K_2NiF_4 lattice. The variation of the lattice parameter as a function of Sr concentration in the solid oxide solutions (Fig. 4) clearly shows the structural distortion in the K_2NiF_4 lattice (*15*). Nguyen *et al.* characterized three similar structural domains in the solid oxide solutions of La, Sr, and Cu: orthorhombic compounds with La_2CuO_4 structure for $0 < x < 0.1$, tetragonal oxides similar to $LaSrCuO_4$ for $0.1 < x < 1$, and several other superstructures derived from the tetragonal cell for $1 < x < 1.34$. They also reported that the compounds corresponding to $0 < x < 1$ differ from the other oxides by the presence of Cu with two oxidation states, +2 and +3 (*15*):

$$SrO + Cu_{Cu} \rightarrow Sr'_{La} + O_o + Cu'_{Cu}. \qquad (2)$$

Thus, obviously two opposite effects which are competitive could be seen in the solid oxide solutions by the substitution of Sr^{2+} for La^{3+}. For small values of x the oxygen vacancies formed at low oxygen pressures are randomly distributed on the oxygen sublattice to preserve the stoichiometric structure La_2CuO_4, but these are filled with the accompanying formation of positive holes at 1 atm oxygen pressure. At higher values of x these oxygen vacancies are probably not completely filled at this oxygen pressure and are ordered or associated with positive holes.

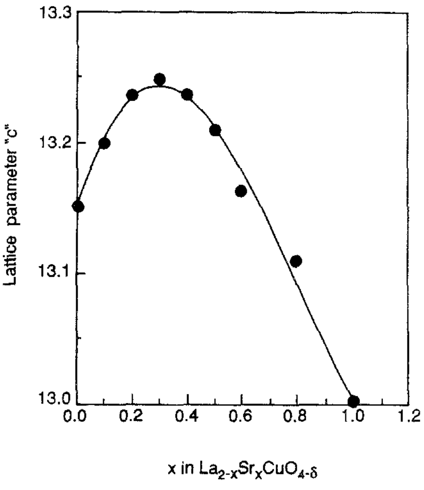

FIG. 4. Lattice parameter as a function of Sr concentration in $La_{2-x}Sr_xCuO_{4-\delta}$.

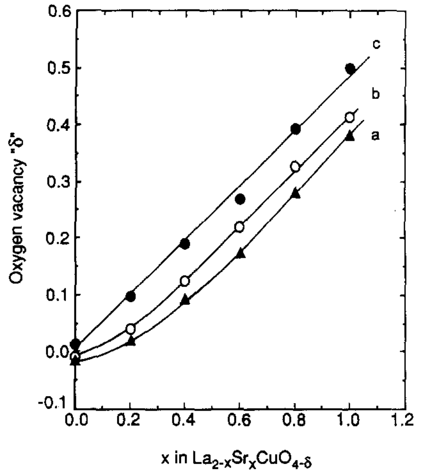

FIG. 5. Variation of oxygen vacancy as a function of Sr concentration in $La_{2-x}Sr_xCuO_{4-\delta}$, (a) $T = 1023$ K, $P_{O_2} = 10^5$ Pa; (b) $T = 1023$ K, $P_{O_2} = 6.6$ Pa; and (c) $T = 1323$ K, $P_{O_2} = 6.6$ Pa.

The overall effect of incorporation of Sr^{2+} in the La^{3+} position is thus represented as

$$SrO + z\,Cu_{cu} \rightarrow Sr'_{La} + O_o + z\,Cu' \cdot Cu + (1 - z)/2\,V''_o. \quad (3)$$

Further increase in x leads to the formation of microphases favoring Cu^{2+} with smaller coordination. Some results of the variation of oxygen vacancy (δ) as a function of Sr^{2+} concentration studied by thermogravimetric analysis are given in Fig. 5. Line c in Fig. 5 shows a linear dependence of δ with x which corresponds to the nominal stoichiometric composition $La^{3+}_{2-x}Sr^{2+}_xCu^{2+}O^{2-}_{4-x/2}$. Lines a and b show deviation from this oxygen stoichiometry at different temperatures. A slow increase in δ was observed with Sr concentration in the range $0 < x < 0.4$, while a linear dependency was obtained for values of x larger than 0.4. Routbort *et al.* observed a decrease in the oxygen diffusion coefficient with increasing Sr addition in these solid solutions, contrary to the expectation that the diffusion coefficient should increase with increasing vacancy concentration caused by the addition of Sr^{2+} (*16*). They explained the observed deviation by the ordering of the oxygen vacancies by binding to Sr clusters at a higher Sr concentration. The initial increase in the oxygen diffusion coefficient with Sr addition could be due to the high mobility of oxygen defects in the dilute solid solutions of Sr, whereas the decrease in the diffusion coefficient after $x = 0.4$ may be due to the low oxygen mobility as a result of ordering of defects in the solid oxide solutions.

The variation of thermodynamic activity of SrO (a_{SrO}) as a function of Sr concentration in these solid oxide solutions is shown in Fig. 6. It can be seen that a_{SrO} increases rapidly with x in the range $0 < x < 0.6$ and then decreases slowly with further increase of x ($0.6 < x < 1.0$). This dependence approximately parallels the catalytic activity for CO oxidation.

Meenakshisundaram *et al.* (*17*) have reported such a volcano plot for CO oxidation on $ZnMn_2O_4$ wherein a small addition of Co^{2+} increases the catalytic activity by providing a highly active Co^{2+} in an octahedral position as these sites are electronically isolated, so that there is a high electron availability for the catalytic reaction. Increase in Co^{2+} concentration, however, causes electron delocalization and hence the absorption of CO as CO^+ is difficult. A subsequent

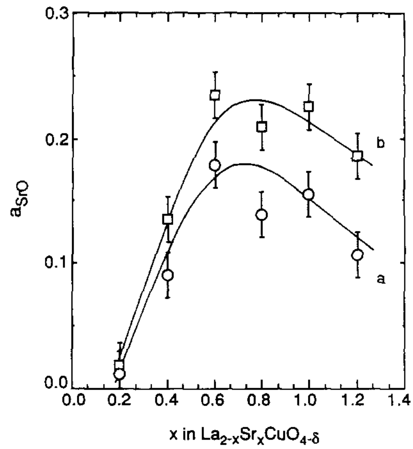

FIG. 6. Variation of thermodynamic activity of SrO as a function of Sr concentration in $La_{2-x}Sr_xCuO_{4-\delta}$ at (a) 1050 K and (b) 1150 K.

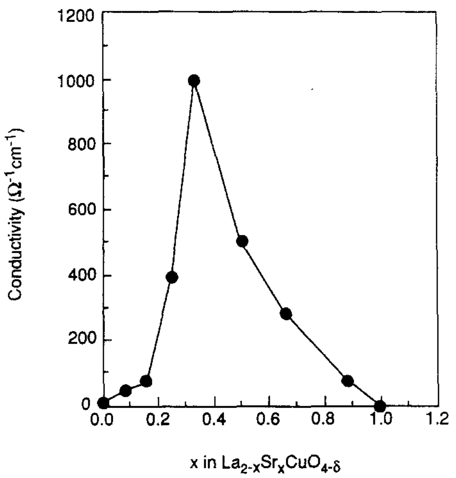

FIG. 7. Variation of electrical conductivity as a function of Sr concentration in $La_{2-x}Sr_xCuO_{4-\delta}$.

increase may be due to the increase in Co^{2+} sites, which also changes the mode of adsorption of CO as a carbonate species. In our case, an increase in Sr at small values of x creates more isolated oxygen defects as well as oxidation of Cu^{2+} to Cu^{3+}. The reactivity of Cu^{3+} could be more than Cu^{2+} since it has the d^8 electronic configuration which is less stable than the d^9 configuration in the Cu^{2+} system. It was also known that the chemisorption for catalytic transformation (reactivity) is proportional to the percentage "d" character in the transition metal series, which is actually a measure of the metallic bond strength. Our observation shows that Cu^{2+} is a very active phase for the carbon monoxide oxidation. Also, none of the solid solutions is more active than CuO. It is therefore possible that the presence of Cu^{2+} as well as the postulated Cu^{3+} accounts for catalytic activity of the solid solutions. It is also interesting to note that the presence of maximum Cu^{3+} at the Sr concentration 0.33 was observed by Nguyen *et al.* in these solid solutions (*18*). Nguyen *et al.* reported that a progressive evolution of the conductivity (of samples quenched from 1273 K in air) from a semiconductor to a semimetallic behavior was obtained as Sr concentration was increased. The conductivity of these solid solutions at 475 K is plotted as a function of Sr concentration (data obtained from Nguyen *et al.* (*18*)) in Fig. 7. Similar volcano behavior is seen in the conductivity of the solid solutions. The formation of Cu^{3+} was deduced by these authors from the Seebeck coefficient, magnetic susceptibility, and conductivity measurements. The increase in the metallic nature of the solid solution may increase adsorption of the precursor reactive species. Thus when the conductivity is maximum we get the maximum catalytic activity and the catalytic activity decreases as the conductivity decreases. At the higher concentration of Sr it is possible that the Sr^{2+}–positive hole association reduces the concentration of catalytic active sites involving oxygen vacancies. Vickerman *et al.* observed a similar volcano effect for the oxychlorination reaction in the solid solutions of $MgAl_2O_4$ while adding Cu (*19–21*). They compared the trend of the catalytic activity with the conductivity of the solid solutions and concluded that the initial increase in the catalytic activity is due to the formation of isolated sites involving Cu pairs in the di-

TABLE 1

Activity of the Oxidation Catalysts for CO Oxidation

Catalyst	La/(La + Sr)	Activity (Temperature °C at CO conversion, %)		
		25%	50%	75%
$CuSrO_2$	0	197	227	242
$LaSrCuO_{4-\delta}$	0.5	187	212	252
$La_{1.6}Sr_{0.4}CuO_{4-\delta}$	0.8	172	192	202
$La_{1.8}Sr_{0.2}CuO_{4-\delta}$	0.9	192	202	227
$La_{1.9}Sr_{0.1}CuO_{4-\delta}$	0.95	177	201	212
La_2CuO_4	1.0	197	240	257
CuO	—	127	146	159
La_2O_3	—	137	192	227
SrO	—	197	244	252

Note. Flow rate 100 ml/min of 1% CO in oxygen at normal temperature and pressure. Weight of Pt/Al_2O_3 catalyst = 0.12 g, that of other catalysts = 0.25 g.

lute Cu solid solutions, and the decrease in the activity with further addition of Cu was due to the delocalization of the electron in the solid solutions. Vickerman *et al.* (*20, 21*) reported a similar trend in nitrous oxide decomposition in a series of solid solutions of α-$Cr_xAl_{2-x}O_3$ and a hydrogen–deuterium exchange reaction in a solid solution of $MgAl_{2-x}Cr_xO_4$. Cimino and co-workers (*22, 23*) observed a similar effect for the solid oxide solutions for a variety of reactions. They also correlated the conduction behavior with the activity in the region "a" due to electronically isolated centers. The activity fall in the region "b" may be a consequence of charge transfer between these sites in the bulk (or polaron hopping). The possibility of charge transfer to an adsorbing molecule is thus reduced. The behavior in the region "c" was thought to be due to the generation of new electron exchange coupled sites.

Such volcano behavior in the catalytic systems was predicted in catalysis by Sabatier, due to the need for the optimum reactant-solid interaction for the higher reactivity (*24*). A weak bond does not allow strong adsorption and the strong bond does not lead to desorption of the product. In the case of formic acid decomposition on metals, Boudart has displayed this volcano behavior where said activity is related to the activity as a function of heat of formation (*25*), which is a measure of metal chemisorptive bond strength.

CONCLUSIONS

The solid oxide solutions of Sr, La, and Cu are quite active catalysts for the oxidation of CO in the temperature range for the pollution abatement studies. The maximum activity with the optimum concentration of Sr in these solid solutions may be due to the formation of active centers which facilitate adsorption, reaction, and desorption in the heterogeneous catalyzed CO oxidation reaction. With the cited evidence from the conductivity, lattice parameter variation, oxygen defect concentration, and strontium oxide activity concomitant with the catalytic oxidation reaction, we conclude that the initial rise in the activity is due to positive hole (Cu^{3+}) formation which may provide a favorable environment for the adsorption of CO and O_2 in the CO oxidation reaction. The subsequent decrease in catalytic activity is due to the formation of ordered oxygen vacancies which also reduce the mobility of the positive holes and hence the conductivity.

Additional studies are, of course, warranted, in particular, selective chemisorption and adsorption heat measurements as a function of Sr composition in these quite provocative solid oxide solutions, which promise not only activity but selectivity behavior to rival traditional metals and their alloys.

ACKNOWLEDGMENT

J. J. C. and S. R. are indebted to the Mobil Oil and Exxon Education Foundation for support of our catalysis studies.

Note added in proof. Since this paper was written, some new evidence, obtained by neutron diffraction (J. D. Jorgensen, Private Communication), suggests that phase separation can occur in the composition range $x = 0.2$–0.5. This is different from the less-sensitive X-ray data obtained in the present study which confirmed published X-ray data suggesting complete miscibility (*26–28*). It now appears that the presence or absence of immiscibility depends on the method of preparation, most significantly on the sintering cycle both with respect to rate of heating and to the final temperature achieved. The procedure used in this study although appearing to be satisfactory according to the present state of knowledge, will be submitted to examination by neutron diffraction analysis in the near future.

REFERENCES

1. Carberry, J. J., Rajadurai, S., Alcock, C. B., and Li, B., *Catal. Lett.* **4,** 43 (1990).
2. Rumpf, F., Poppa, H., and Boudart, M., *Langmuir* **4,** 722 (1988).
3. Yao-En, Li, Boecker, D., and Gonzalez, R. D., *J. Catal.* **110,** 319 (1988).
4. Plath, P. A., Moeller, K., and Jaeger, N. I., *J. Chem. Soc. Faraday Trans. 1* **84,** 1751 (1988).
5. Sant, R., and Wolf, E. E., *J. Catal.* **110,** 249 (1988).
6. Voorhoeve, R. J. H., Johnson, Jr., D. W., Remeika, J. P., and Gallagher, P. K., *Science* (*Washington, D.C., 1883–*) **195,** 827 (1977).

7. McCarthy, E., Zaahradnik, J., Kuczynski, G. C., and Carberry, J. J., *J. Catal.* **39,** 29 (1975).
8. Boudart, M., and Rumpf, F., *React. Kinet. Catal. Lett.* **35,** 95 (1987).
9. Libby, W. F., *Science (Washington, D.C., 1883–)* **171,** 499 (1971).
10. Peedersen, L. A., and Libby, W. F., *Science (Washington, D.C., 1883—)* **176,** 1355 (1972).
11. Voorhoeve, R. J. H., Rameika, J. P., Freeland, P. E., and Matthias, B. T., *Science (Washington, D.C., 1883–)* **177,** 353 (1972).
12. Serrano, C., and Carberry, J. J., *Appl. Catal.* **19,** 119 (1985).
13. Alcock, C. B., and Li, B., *J. Am. Ceram. Soc.*, **73,** No. 5 1176 May (1990).
14. Li, B., Ph.D. Dissertation, University of Notre Dame, 1990.
15. Nguyen, N., Choisnet, J. Hervieu, M. V., and Raveau, B., *J. Solid State Chem.* **39,** 120 (1981).
16. Routbort, J. L., Rothman, S. J., Flandermeyer, B. K., Niwicki, L. J., and Baker, J. E., *J. Mater. Reson.* **3** 116 (1988).
17. Meenakshisundaram, A., Gunasekaran, G., and Srinivasan, V., *in* "Advances in Catalysis Science and Technology" (T. S. R. Prasuda Rao, Ed.), Proceedings, 7th National Symposium on Catalysis, Baroda, p. 723. Wiley, New Delhi, 1985.
18. Nguyen, N., Studer, F., and Raveau, B., *J. Phys. Chem. Solids 44,* 389 (1983).
19. Egerton, T. A., Stone, F. S., and Vickerman, J. C., *J. Catal.* **33,** 299 (1974).
20. Vickerman, J. C., *J. Catal.* **44,** 404 (1976).
21. Sharp, P. K., Vickerman, J. C., and Stacey, M. H., "Proceedings, 6th International Congress Catalysis, London, 1976," p. 225. (G. C. Bond, P. B. Wells, and F. C. Thomkins, Eds.). The Chemical Society, London, 1977.
22. Cimino, A., Indovina, V. Pepe, F., and Schiavello, M., *J. Catal.* **14,** 49 (1969).
23. Cimino, A., and Indovina, V., *J. Catal.* **17,** 54 (1970).
24. Carberry, J. J., *in* "Chemical and Catalytic Reaction Engineering," p. 433. McGraw–Hill, New York, 1976.
25. Boudart, M., *Chem. Eng. Prog.* **57,** 33 (1961).
26. Kitaguchi, H., *et al., J. Ceram. Soc. Jpn.* **96,** 388 (1988).
27. De Leeuw, D. M., Mutsaers, C. A. H. A., Geelen, G. P. J., and Langereis, C., *J. Solid State Chem.* **80,** 276 (1989).
28. Hahn, J., *et al., Chemtronics* **2,** 126 (1987).